Hindawi Publishing Corporation
Shock and Vibration
Volume 2015, Article ID 502747, 9 pages
http://dx.doi.org/10.1155/2015/502747

Research Article

Thermodynamic Behaviors of a Kind of Self-Decoupling Magnetorheological Damper

Guojun Yu,[1] Chengbin Du,[2] and Tiger Sun[1]

[1]*Faculty of Civil Engineering and Mechanics, Jiangsu University, Zhenjiang, Jiangsu 212013, China*
[2]*Department of Engineering Mechanics, Hohai University, Nanjing 210098, China*

Correspondence should be addressed to Tiger Sun; ts420@ujs.edu.cn

Received 8 January 2015; Accepted 27 March 2015

Academic Editor: Weihua Li

A theoretical model of temperature change on a kind of self-decoupling magnetorheological (SDMR) damper was established based on conservation of energy, and the constraint equation for structural design parameters of the SDMR damper was improved to satisfy heat dissipation requirements in this work. According to the theoretical model and improved constraint equation, the main structure parameters of SDMR damper were obtained and the damper was tested. The temperature performance test results indicate that the rising temperature makes the damping force decline, and the main affection factors of temperature variation are excitation methods and input current. The results also show that the improved constraint equation and design method introduced are correct and efficient in the engineering.

1. Introduction

The magnetorheological (MR) damper is an excellent and controllable damper based on MR intelligent materials [1–4]. Its biggest advantage is that a computer can be used to adjust the parameters automatically according to the structure's vibration response [5, 6], thus achieving the best effect for the intelligent control of structure vibration. MR dampers using civil engineering structure control have large stress amplitude and sudden change in work current [7, 8], therefore making the energy caused by an earthquake or wind vibration convert more internal heat. Thus, the working temperature of MR damper increases greatly in a short time, which is a topic rarely studied both in the country and abroad. Goncalves and Ahmadian [9] studied the energy dissipated in an MR damper for semiactive vehicle suspensions and recognized that there is a decline in the performance of the damper due to temperature changes. Liu et al. [10] studied semiactive suspension control of a High Mobility Multipurpose Wheeled Vehicle (HMMWV) using the fail-safe MR damper; the results indicate that temperature changes greatly influence the performance of the suspension system. Gordaninejad and Kelso [11] analysed the effect of heat transfer when the damper used in off-highway, high-payload vehicles, and a fluid-mechanics-based theoretical model along with a 3D finite element electromagnetic analysis is utilized to predict the MRF damper performance. Dogrouz et al. [12, 13] presented a lumped system model for predicting the heat transfer from fail-safe MR fluid dampers, and the results show that the model slightly overpredicts the temperature rise when compared to experimental data, the heat transfer can be considerably enhanced with the use of the fins, and both the mechanical and electrical power input contribute substantially to the temperature rise. Ramos et al. [14] presented a model to predict the thermal performance of automotive twin-tube shock absorbers simulating a thermal stability test. To get a better correlation between the model and the experimental results, it was proposed that the temperatures of the internal components of the shock absorber are measured to adjust the coefficients of the internal convection correlations. Batterbee and Sims [15] considered temperature sensitive controller performance of MR dampers. A dynamic temperature-dependent model of an MR damper was first developed and validated. Wilson and Wereley [16] presented a physically motivated model to capture the MR damper behavior, including the contributions of fluid and pneumatic stiffness of the damper realized at high piston velocity. The effect of damper self-heating

on the model parameters was investigated and the trends with temperature variation are presented. Marr et al. [17] developed a nonlinear, temperature-dependent model, which demonstrates the ability to capture trends in both frequency and dynamic displacement for both the storage and loss moduli over a range of frequencies (0.35 Hz–15 Hz), a range of displacements (0.005 in–0.3 in), and a range of temperatures (−40°F–140°F). The model is able to predict the more pronounced nonlinearities at the higher frequencies, higher displacements, and large temperature changes. Black and Makris [18] summarized the results from a comprehensive experimental program in an effort to better understand the phenomenon of viscous heating of fluid dampers under small-stroke (wind loading) and large-stroke (earthquake loading) motions. The study presents a valuable formula that can be used in practice to estimate the internal fluid temperature of the damper given the external shell temperature.

The existing MR dampers are designed for the linear vibration of structures; the damping effect is obvious for the structure of weak nonlinearity. When MR dampers are installed within the skeleton of buildings to suppress the low degree earthquakes or wind-induced vibrations, the piston displacements and velocities are relatively small. In contrast, there are a lot of the strong nonlinear behaviors in actual structures when strong earthquakes occur; the MR dampers are incorporated either in the seismic isolation system of structures or between the towers/peers and the deck of bridges; the piston displacements and velocities can be large [18]. The damper design for the application of nonlinear structure has become an important research field. MR dampers suppress the kinetic energy of structures into heat. When the dampers undergo large displacement histories and small but prolonged displacement histories, the temperature rise within the MR fluid of the damper might be appreciable to the extent that it may damage the damper.

This work presents a comprehensive experimental study on the problem of viscous heating of MR dampers. We developed a self-decoupling magnetorheological (SDMR) damper with a 360 KN maximum damping force and the SDMR damper is suitable for the vibration control of nonlinear civil engineering structures, and it consists of self-decoupling device which is activated depending on the structure displacement [19]. The paper explored the influence of temperature changes on the damper performance. We analyzed the temperature change when the damper is at work to provide theoretical basis for valuable formula modeling and simulation and for further experimental research.

2. Design Principle and Thermodynamics of SDMR Damper

The damping force equation of the SDMR damper is given [19]. Consider

$$F = \frac{3\eta L\left[\pi\left(D_i^2 - d^2\right)\right]^2}{4\pi D_i h^3}\dot{x} + \frac{3L\pi\left(D_i^2 - d^2\right)[1 + J(x)]}{4h}\tau_y \operatorname{sgn}(\dot{x}) + K(x), \tag{1}$$

where

$$J(x) = \begin{cases} \dfrac{x\operatorname{sgn}(\dot{x}) + S - 2x_0}{x_0}, & \\ \qquad -S \le x\operatorname{sgn}(\dot{x}) \le x_0 - S & \\ -1, \quad x_0 - S \le x\operatorname{sgn}(\dot{x}) \le x_0 + x_1 - S & \\ \dfrac{x\operatorname{sgn}(\dot{x}) + S - 2x_0 - x_1}{x_0}, & \\ \qquad x_0 + x_1 - S \le x\operatorname{sgn}(\dot{x}) \le 2x_0 + x_1 - S & \\ 0, \quad 2x_0 + x_1 - S \le x\operatorname{sgn}(\dot{x}) \le S & \end{cases}$$

$$K(x) = \begin{cases} kx\operatorname{sgn}(x)\operatorname{sgn}(\dot{x}), & S \le C \\ -kx, & x\operatorname{sgn}(\dot{x}) < C - S,\ S > C \\ kx, & C - S < x\operatorname{sgn}(\dot{x}) < 2C - S,\ S > C \\ 0, & x\operatorname{sgn}(\dot{x}) > 2C - S,\ S > C, \end{cases} \tag{2}$$

where F is the damping force, L is the effective length of the piston, D_i is the cylindrical inner diameter, d is the diameter of the rod, h is the size of the working space, v is the piston velocity, τ_y is the yield stress of the MRF, and η is the off-state viscosity of the MRF. S is the amplitude, x_0 is the absolute value of the critical displacement for the delay, x_1 is the empty trip of the damper, C is the maximum compression of the spring, and k is the spring elastic constant. $\eta = \eta_0 e^{-\lambda(T-T0)}$, where η and η_0 are the viscosity of the MR fluid at T and T_0 and λ is the viscosity-temperature coefficient. The changes in the damping magnetic field depend on the changes in the current, relative magnetic conductance, resistivity, and the material's specific heat while the temperature is changing [20].

For the MR damper, the main sources of heat are liquid damping, friction, and magnetic coil. When used under general conditions, the heat caused by friction is usually lesser than that caused by liquid damping, and we assume that the energy dissipation in the MR damper work process includes only the liquid damping and magnetic coil. The energy balance equation of MR damper is given by

$$W_1 + W_2 - Q = \Delta U. \tag{3}$$

The work done when the damper dissipates external input energy is

$$W_1 = F \cdot X(t). \tag{4}$$

Using (4), (1) becomes

$$W_1 = \left\{ \frac{3\eta L\left[\pi\left(D_i^2 - d^2\right)\right]^2}{4\pi D_i h^3}\dot{x} + \frac{3L\pi\left(D_i^2 - d^2\right)[1 + J(x)]}{4h} \cdot \tau_y \operatorname{sgn}(\dot{x}) + K(x) \right\} \cdot X(t). \tag{5}$$

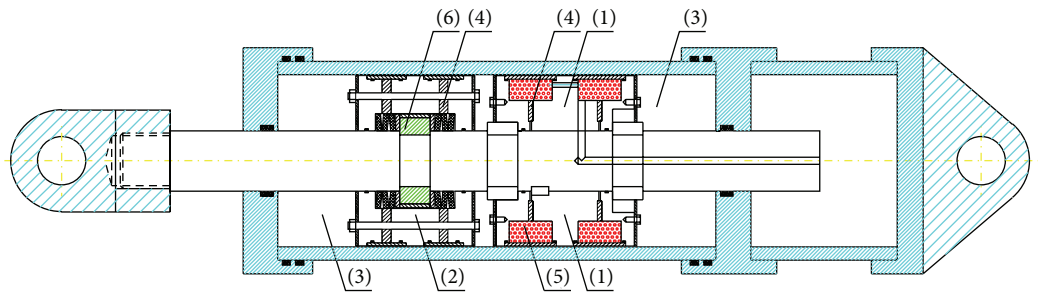

Figure 1: Structure of the SDMR damper.

According to Ohm's Law, the heat generated by the damper field coil is

$$W_2 = I^2(t)\,Rt, \tag{6}$$

where t is time.

According to the theory of heat conduction, the heat exchange between the damper and the environment outside the damper is

$$Q = \alpha A\left(T - T_0\right)t, \tag{7}$$

where A is the damper's total heat area given by

$$A = \left(\frac{\pi D^2}{2} + \pi Dl\right). \tag{8}$$

And α is the damper's coefficient of total heat dissipation. Considering comprehensively the convection, radiation, and effect of heat transfer, α can be written as [21]

$$\alpha = \frac{4v_0^{0.7}}{D^{0.3}} + \varepsilon\sigma_b\left(\frac{T_a^4 - T_{a0}^4}{T_a - T_{a0}}\right). \tag{9}$$

Using (5)–(9), (3) becomes

$$\begin{aligned}&\left\{\frac{3\eta L\left[\pi\left(D_i^2 - d^2\right)\right]^2}{4\pi D_i h^3}\dot{x}\right.\\&\left.+\frac{3L\pi\left(D_i^2 - d^2\right)\left[1 + J(x)\right]}{4h}\tau_y\,\mathrm{sgn}(\dot{x}) + K(x)\right\}\\&\cdot X(t) + I^2(t)\,Rt - \left[\frac{4v_0^{0.7}}{D^{0.3}} + \varepsilon\sigma_b\left(\frac{T_a^4 - T_{a0}^4}{T_a - T_{a0}}\right)\right]\\&\cdot\left(\frac{\pi D^2}{2} + \pi Dl\right)\cdot\left(T - T_0\right)t = \Delta T\cdot C_{\mathrm{sum}},\end{aligned} \tag{10}$$

where ΔU is the internal energy dissipation that causes temperature changes in the damper, X is the exerting displacement, v_0 is the relative velocity of air, ε is the blackening coefficient of the outside wall, l is the length of the work cylinder, $\sigma_b = 5.67 \times 10^{-8}$ is the radiation constants of the absolute blackbody [21], T_a and T_{a0} are the absolute temperatures at T and T_0, respectively, C_{sum} is the entire heat capacity of the damper, and ΔT is the temperature change of the damper.

3. Design of SDMR Damper

3.1. Structural Design. The SDMR damper in this paper, as shown in Figure 1, is a kind of damper used in civil engineering structures for antivibration, specifically an antivibration device with damping force decoupling characteristics and protection from self-invalidation. The damper's stiffness and damping characteristics are very sensitive to the incentive's frequency and amplitude. It has a relatively small damping force in the case of small amplitudes and a large damping force in the case of large amplitudes, and the damping force can be adjusted; thus, the damper can effectively reduce the structure's reaction to various vibration excitations and has good stability and invalidation protection. The core work parts are the main piston (1) and the two subpistons (2), the work cylinder filled with MR fluid (3), the main piston ring with a permanent magnet (4) and magnetic coil (5), and the permanent magnet self-decoupling baffle in the subpiston magnetizer (6).

The SDMR damper is mainly used in building structures; therefore, large and small displacements in the damper design are 60 mm and 5 mm, respectively. The existing MR dampers are designed for the linear vibration of structures; the damping effect is obvious for the structure of weak nonlinearity. When MR dampers are installed within the skeleton of buildings to suppress the low degree earthquakes or wind-induced vibrations, the piston displacements and velocities are relatively small. Therefore, a damper with a small damping force is required for vibration control. The core work part of the SDMR damper is the main piston (1). In contrast, there are a lot of the strong nonlinear behaviors in actual structures when strong earthquakes occur; the MR dampers are incorporated either in the seismic isolation system of building structures or between the towers/peers and the deck of bridges; the piston displacements and velocities can be large. Therefore, a damper with a large damping force is better for vibration control. The core work parts of the SDMR damper are the main piston (1) and the two subpistons (2).

3.2. Magnetic Circuit Design. The basic principle of a SDMR damper can be described as the permanent magnet and magnetic coil in the main piston magnetic circuit with the excitation magnetic field and the permanent magnetic field. The coil used wounds inwards, and two coils are placed in parallel. The current magnetic field of the coil can strengthen

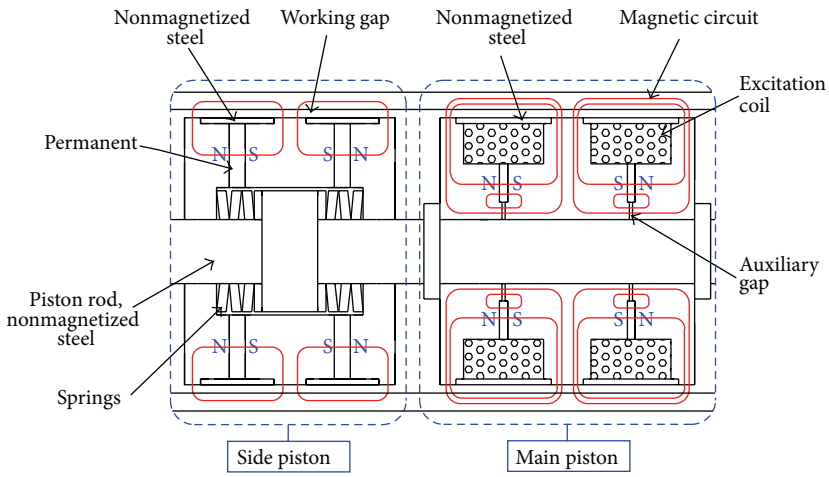

Figure 2: Flux lines of the SDMR damper.

or weaken the magnetic field of the permanent magnet in the damping channel [22]. In the subpiston, we set only the permanent magnet. The distribution of magnetic flux lines is shown in Figure 2.

The permeable magnetic material adopted is steel 45#, and the permanent magnetic material adopted is no. 30 NdFeB. In addition, with the introduction of a permanent magnet in the magnetic structure, even in the case of a loss of external energy, the damper can still guarantee a larger damping force. It overcomes the dependence of the traditional MR damper on the external energy. As mentioned previously, the damper is suitable for vibration control of civil engineering structures.

3.3. Temperature Effect on MR Viscosity and Magnetic Circuit. To achieve the purpose of reducing the vibration, the vibration energy of the SDMR damper translates into heat energy stored in the interior of the damper. Parts of the heat dissipate through the cylinder wall into the air through convection, conduction, and radiation, whereas other parts remain and increase the temperature in the form of internal energy to obtain a balance temperature.

The damping force includes the viscous damping force and the Coulomb damping force. The viscous damper is only related to the speed and viscosity of the MR fluid, $\eta = \eta_0 e^{-\lambda(T-T0)}$, where λ is the viscosity-temperature coefficient. The trend of the SDMR damper's viscidity is presented in Figure 3. The changes in the Coulomb damping force depend mainly on the magnetic field changes, whereas the changes in the magnetic field depend on the changes in current, relative magnetic conductance, resistivity, and the material's specific heat during temperature changes. The relationship curve between the MR fluid shear yield strength and the magnetic field intensity is shown in Figure 4, whereas the relationship among the relative magnetic conductance, specific heat, and resistivity of 45# steel with the temperature changes is shown in Table 1 [23].

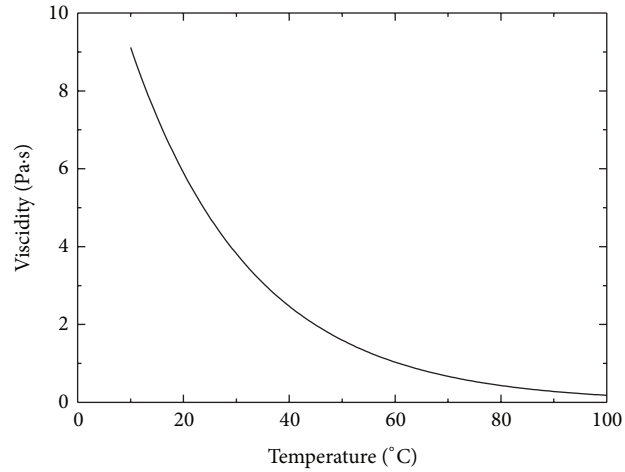

Figure 3: Variety trend of SDMR damper's viscidity.

3.4. Optimization Parameter. The temperature increase of the MR fluid is not unlimited when the MR damper is at work. The damper needs to obtain thermal balance when the temperature is critical. Therefore, in the damper design, the allowable working temperature must be considered to prevent exorbitant temperature that leads to failure.

The allowable temperature of the MR damper depends on the following three aspects: (1) flash points of the temperature of the MR fluid, (2) stable boundary temperature of the damper sealing material, and (3) allowable temperature that satisfies the damper performance requirements, namely, the temperature when the damper's rated typical set-point damping force declines to the limit because of the increase in working temperature. The temperature should no longer increase when the damper reaches the allowable temperature, and at this time the heat dissipation and outside work should be the same as in (3). The dissipated heat when the damper reaches its allowable temperature, T_x, is $\Delta T \cdot C_{\text{sum}}$.

Table 1: Temperature properties of 45# steel.

Temperature (°C)	Resistivity ($\times 10^{-7}$ Ω·m)	Permeability	Specific heat (J·(kg·K)$^{-1}$)
0	1.84	300	470
80	2.35	295	480
160	2.86	290	500
240	3.84	282	520
320	4.72	275	540
400	5.58	268	550

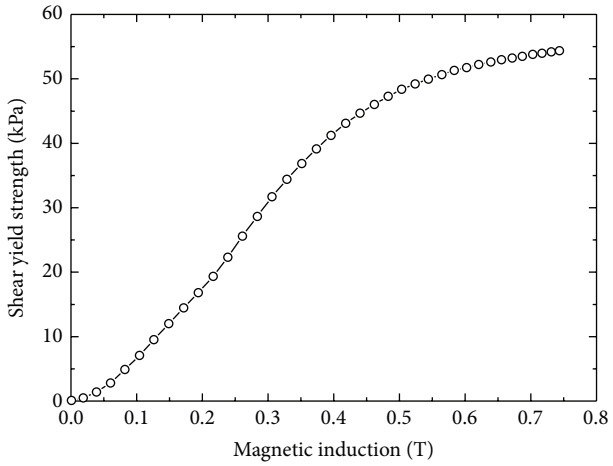

Figure 4: Curve between shear stress and magnetic induction.

Figure 5: The photo of SDMR damper.

Considering the effect of viscosity-temperature coefficient on the viscous damping force and that of temperature on the relative magnetic conductance resistivity of the damper magnetic materials, which influence the magnetic induction intensity of damping clearances, we can define the Coulomb force attenuation coefficient ζ, resistance coefficient δ, and heat coefficient φ. Thus, with (10), we can calculate the allowable temperature using the following equation:

$$\begin{aligned}&\left\{\frac{3\eta_0 e^{-\lambda(T_x-T_0)}L\left[\pi\left(D_i^2-d^2\right)\right]^2}{4\pi D_i h^3}\dot{x}\right.\\&\left.+\frac{3\zeta L\pi\left(D_i^2-d^2\right)[1+J(x)]}{4h}\tau_y\,\mathrm{sgn}(\dot{x})+K(x)\right\}\\&\cdot X(t)+\delta I^2(t)Rt-\left[\frac{4v_0^{0.7}}{D^{0.3}}+\varepsilon\sigma_b\left(\frac{T_a^4-T_{a0}^4}{T_a-T_{a0}}\right)\right]\\&\cdot\left(\frac{\pi D^2}{2}+\pi Dl\right)\cdot(T_x-T_0)t=\Delta T\cdot\varphi\cdot C_{\mathrm{sum}}.\end{aligned}\tag{11}$$

With these operating conditions, we can design the damper's heat-radiating parameters when the allowable temperature of the MR damper is decided. The improved constraint equations can also be used as constraint conditions for the heat dissipation factors in the structural design process. After repeatedly adjusting the design parameters, we finally confirmed that the main thermal parameters of the damper include the damper outside wall thickness, ε, the cylinder's external diameter, D, and the cylinder length, l. The main parameters of the final damper design are shown in Table 2, $L = L_m + L_s$, and the SDMR damper is shown in Figure 5.

4. Temperature Characteristic Test of the SDMR Damper

To validate the rationality and feasibility of the SDMR damper design and study the one performance, we conducted a temperature characteristic test on the electrohydraulic servo-dynamic-static tester (SDS-300) at the Material Mechanics Laboratory of the Mechanics Experimental Centre of Hohai University. The experimental setup of the SDMR damper is shown in Figure 6. The test uses displacement control method, with the sine curve as the input. The test cases are presented in Table 3. When the current values of cases are 0 A, the damper can still guarantee a larger damping force under the magnetic field produced by the permanent magnet.

5. Results and Discussion

The test environment temperature is 28.8°C using the TES1327 K infrared thermometer to measure the temperature of the damper's external cylinder. Figures 7 and 8 show the time process of the SDMR damper temperature variation

Table 2: Main structural parameters of the SDMR damper.

Main structural parameters	Coefficient	Unit	Value
Initial MRF viscosity	η	Pa·s	4.7
MRF yield strength	τ_y	kPa	54
Work clearances	h	mm	1.2
Cylinder external diameter	D	mm	230
Cylinder inner diameter	D_i	mm	200
Piston pod diameter	d	mm	70
Spring effective itinerary	C	mm	5
Main piston work channel length	L_m	mm	40
Total length	l	mm	996
Force range of small itinerary	F	kN	16.1~195.7
Force range of large itinerary	F	kN	195.7~362.2
Coil circle number	n	—	800
Entirety heat capacity	C_{sum}	kJ·(K)$^{-1}$	427.5
Critical temperature	T	°C	100
The maximum power	P	W	<100
Current range	I	A	−2~2
Subpiston work channel length	L_s	mm	40
Coil total resistance	R	Ω	23.8
Blackening coefficient of the outside wall	ε	—	0.95
The Coulomb force attenuation coefficient	ζ	—	0.93–0.95
Resistance coefficient	δ	—	0.98–0.99
Heat coefficient	φ	—	0.91–0.94

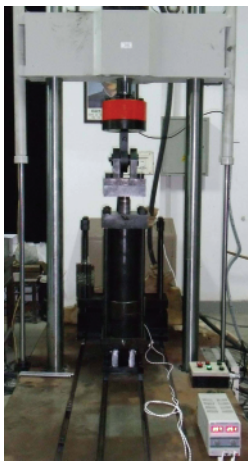

Figure 6: Experimental setup of a SDMR damper.

Table 3: MR damper temperature performance test cases.

Case	Current (A)	Amplitude (mm)	Frequency (Hz)
1	0	5	0.5
2	2	5	0.5
3	2	5	1.3
4	0	60	0.1

for the four cases. We selected case 4 to draw the hysteretic curve of the damping force as it changed with temperature,

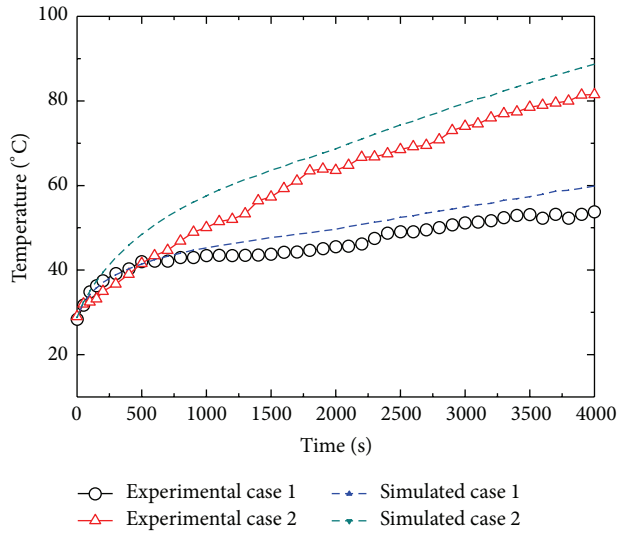

Figure 7: Various temperatures of an MR damper with case 1 and case 2.

as shown in Figure 9. Table 4 presents the test results of the damping characteristics affected by temperature.

From the above test results, we can obtain the following conclusions.

(1) In Figures 7 and 8, the temperature of the MR damper changes while it is at work, which is roughly a linear change. The main influencing factors for the damper

Table 4: Test results of the MR damper characteristics.

Case	Highest temperature (°C)	Range of temperature (°C)	Damping force change (kN)	Damping reduction (%)
1	53.8	25.4	117.3~109.4.1	6.73
2	81.5	52.5	169.8~157.9	7.01
3	95.5	67.1	178.1~167.5	5.95
4	99.1	70.3	297.7~275.1	7.59

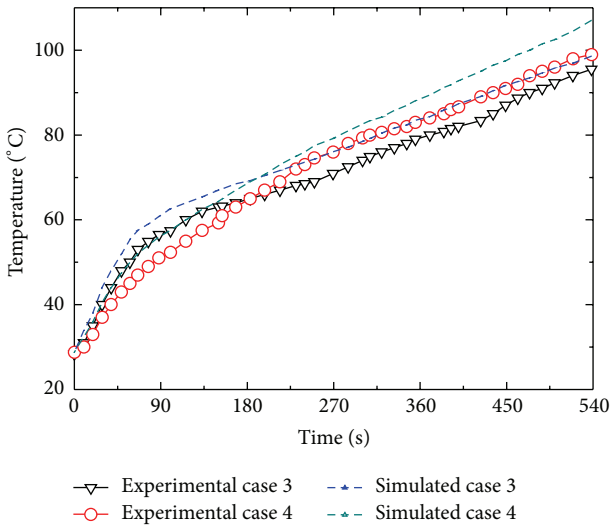

Figure 8: Various temperatures of an MR damper with case 3 and case 4.

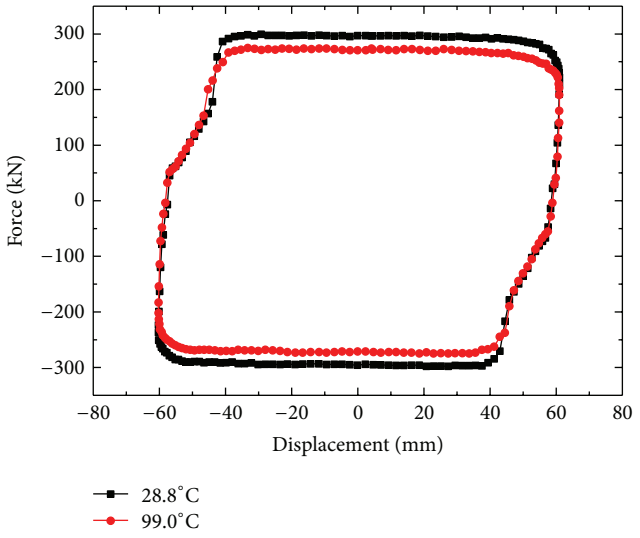

Figure 9: Curves of damper force changes with respect to temperature.

temperature changes are incentive methods and work current. Comparing the curves of the temperature changing with time for cases 1 and 2 in Figure 7, in certain frequencies and amplitudes, the temperature of case 2 that switches with the current rises faster than the temperature of case 1, which shows an obvious effect of the current.

(2) Under the case of switching on the current and changing the incentive, the temperature curve of the damper becomes flat after 4000 s, consistent with the theoretical calculation. Comparing the theoretical and measured curves in Figures 7 and 8, the measured value is slightly lower than the theoretical value, due to the fact that the theoretical value is the internal temperature of the damper and the measured value is the surface temperature of the damper. Therefore, we can conclude that the MR damper balance temperature can be determined through the parameter design. As the wind excitation time on the building structure is much longer than the earthquake excitation time, the performance of the SDMR damper is important in the use of the wind vibration control in civil engineering.

(3) Comparing the curves of cases 2 and 3 in Figures 7 and 8, the initial temperature rise of the damper in the case of high frequency incentive is faster than that in the case of low frequency incentive.

(4) According to Figure 9 and Table 4, the damping force of the MR damper declines when the temperature rises. For civil engineering, seismic events only occur for dozens of seconds, and the temperature rises by 5°C. The damping force attenuation is so little that we can ignore its influence on civil engineering structures. Thus, the SDMR damper we designed has good temperature stability.

6. Conclusion

As the energy dissipation equipment designed SDMR damper's temperature is changing during the work time which caused damper capability decline. For this reason, the effect of temperature was studied and the following conclusions were obtained.

(1) Based on conservation of energy theory, a theoretical model of temperature change of SDMR damper was established, and the constraint equation for structural design parameters of the MR damper was improved to satisfy heat dissipation requirements.

(2) According to the theoretical model and improved constraint equation, main structure parameters of a SDMR damper were obtained and the damper was tested. The temperature performance test result indicates that the rising temperature makes the damping force decline, and the main affecting factors of

temperature variation are excitation methods and input current.

(3) The key technology research on structure, heat dissipation, and heating behaviour tests of SDMR damper also show that the improved constraint equation and design method introduced are correct and efficient. The temperature of SDMR damper achieves a dynamic balance after 4000 s; the behavior of the SDMR damper is important in the use of the wind vibration control in civil engineering.

(4) The key technology on structure, magnetic circuit, heat dissipation, and temperature characteristic tests of SDMR damper could provide reference for a large-tonnage MR damper in the aspects of reasonable parameter determination, design, and proper manufacturing. It also provides the basis for the nonlinear vibration control design of actual civil building structures that make use of MR dampers.

Conflict of Interests

The authors declare that there is no conflict of interests regarding the publication of this paper.

Acknowledgments

This work was supported by the Natural Science Foundation of Jiangsu Province of China (Grant no. BK20140560), the Research Foundation for Advanced Talents of Jiangsu University (Grant nos. 14JDG161, 14JDG162), and the Jiangsu Province Science and Technology Support Program, China (Grant no. BE2012180).

References

[1] M. Zapateiro, H. R. Karimi, N. Luo, and B. F. Spencer Jr., "Real-time hybrid testing of semiactive control strategies for vibration reduction in a structure with MR damper," *Structural Control and Health Monitoring*, vol. 17, no. 4, pp. 427–451, 2010.

[2] B. J. Park, F. F. Fang, and H. J. Choi, "Magnetorheology: materials and application," *Soft Matter*, vol. 6, no. 21, pp. 5246–5253, 2010.

[3] H. W. Huang, L. M. Sun, and X. L. Jiang, "Vibration mitigation of stay cable using optimally tuned MR damper," *Smart Structures and Systems*, vol. 9, no. 1, pp. 35–53, 2012.

[4] S. N. Madhekar and R. S. Jangid, "Seismic response control of benchmark highway bridge using variable dampers," *Smart Structures and Systems*, vol. 6, no. 8, pp. 953–974, 2010.

[5] S. J. Dyke, B. F. Spencer Jr., M. K. Sain, and J. D. Carlson, "An experimental study of MR dampers for seismic protection," *Smart Materials and Structures*, vol. 7, no. 5, pp. 693–703, 1998.

[6] S.-Y. Ok, D.-S. Kim, K.-S. Park, and H.-M. Koh, "Semi-active fuzzy control of cable-stayed bridges using magneto-rheological dampers," *Engineering Structures*, vol. 29, no. 5, pp. 776–788, 2007.

[7] G. Yang, B. F. Spencer Jr., J. D. Carlson, and M. K. Sain, "Large-scale MR fluid dampers: modeling and dynamic performance considerations," *Engineering Structures*, vol. 24, no. 3, pp. 309–323, 2002.

[8] J. W. Tu, J. Liu, W. L. Qu, Q. Zhou, H. B. Cheng, and X. D. Cheng, "Design and fabrication of 500-kN large-scale MR damper," *Journal of Intelligent Material Systems and Structures*, vol. 22, no. 5, pp. 475–487, 2011.

[9] F. D. Goncalves and M. Ahmadian, "Experimental investigation of the energy dissipated in a magneto-rheological damper for semi-active vehicle suspensions," *American Society of Mechanical Engineers*, vol. 72, no. 1, pp. 459–467, 2003.

[10] Y. M. Liu, F. Gordaninejad, C. A. Evrensel et al., "Temperature-dependent skyhook control of HMMWV suspension using a fail-safe magnetorheological damper," in *Smart Structures and Materials 2003: Industrial and Commercial Applications of Smart Structures Technologies*, vol. 5054 of *Proceedings of SPIE*, pp. 332–340, San Diego, Calif, USA, August 2003.

[11] F. Gordaninejad and S. P. Kelso, "Fail-safe magneto-rheological fluid dampers for off-highway, high-payload vehicles," *Journal of Intelligent Material Systems and Structures*, vol. 11, no. 5, pp. 395–406, 2000.

[12] M. B. Dogrouz, F. Gordaninejad, and A. J. Stipanovich, "An experimental study on heat transfer from fail-safe magneto-rheological fluid dampers," in *Smart Structures and Materials 2001: Damping and Isolation*, vol. 4331 of *Proceedings of SPIE*, pp. 355–369, July 2001.

[13] M. B. Dogrouz, E. L. Wang, F. Gordaninejad, and A. J. Stipanovic, "Augmenting heat transfer from fail-safe magneto-rheological fluid dampers using fins," *Journal of Intelligent Material Systems and Structures*, vol. 14, no. 2, pp. 79–86, 2003.

[14] J. C. Ramos, A. Rivas, J. Biera, G. Sacramento, and J. A. Sala, "Development of a thermal model for automotive twin-tube shock absorbers," *Applied Thermal Engineering*, vol. 25, no. 11-12, pp. 1836–1853, 2005.

[15] D. Batterbee and N. D. Sims, "Temperature sensitive controller performance of MR dampers," *Journal of Intelligent Material Systems and Structures*, vol. 20, no. 3, pp. 297–309, 2009.

[16] N. L. Wilson and N. M. Wereley, "Analysis of a magnetorheological fluid damper incorporating temperature dependence," Technical Paper—51st AIAA/ASME/ASCE/AHS/ASC Structures, Structural Dynamics, and Materials Conference AIAA 2010-2993, 2010.

[17] C. Marr, G. A. Lesieutre, and E. C. Smith, "Nonlinear, temperature-dependent, fluidlastic lead-lag damper modeling," in *Proceedings of the 2008 AHS Annual Forum Proceedings*, vol. 3, pp. 2370–2381, AHS International, 2008.

[18] C. J. Black and N. Makris, "Viscous heating of fluid dampers under small and large amplitude motions: experimental studies and parametric modeling," *Journal of Engineering Mechanics*, vol. 133, no. 5, pp. 566–577, 2007.

[19] C. B. Du, F. X. Wan, and G. J. Yu, "A magnetic flux leakage study of a self-decoupling magnetorheological damper," *Smart Materials and Structures*, vol. 20, no. 6, Article ID 065019, pp. 65–76, 2011.

[20] G. Yu, C. Du, and F. Wan, "Numerical simulation of a self-decoupling magneto-rheological damper on electromagnetic-thermal coupling," *Advanced Materials Research*, vol. 139–141, pp. 2386–2390, 2010.

[21] S. Q. Liu, K. K. Zhou, S. F. Yuan, B. Yao, and Y. S. Jia, "Temperature characteristic of one tube MR damper," *Tractor & Farm Transporter*, vol. 35, no. 2, pp. 14–16, 2008 (Chinese).

[22] W.-M. Yan, J.-B. Ji, B. Dong, and H.-J. Ge, "Theoretical and experimental studies on a new reversible magnetorheological damper," *Structural Control and Health Monitoring*, vol. 18, no. 1, pp. 1–19, 2011.

[23] A. R. Kiani-Rashid, G. I.-A. Bozchalooi, and H. R. Azzat-Pour, "The influence of annealing temperature on the graphitisation of CK 45 Steel," *Journal of Alloys and Compounds*, vol. 475, no. 1-2, pp. 822–826, 2009.